processes

MDPI

Article

Solar Photo-Fenton: An Effective Method for MCPA Degradation

Alicia Martin-Montero [1,*], Argyro Maria Zapanti [2], Gema Pliego [1], Jose A. Casas [1] and Alicia L. Garcia-Costa [1,*]

[1] Chemical Engineering Department, School of Science, Universidad Autónoma de Madrid, Ctra. Colmenar km 15, 28049 Madrid, Spain; gema.pliego@uam.es (G.P.); jose.casas@uam.es (J.A.C.)
[2] Department of Sustainable Agriculture, School of Agricultural Sciences, University of Patras, 30131 Agrinio, Greece; up1065547@ac.upatras.gr
* Correspondence: alicia.martinm@uam.es (A.M.-M.); alicial.garcia@uam.es (A.L.G.-C.)

Abstract

The extensive use of herbicide 2-methyl-4-chlorophenoxyacetic acid (MCPA), coupled with its limited biodegradability, has led to its ubiquitous presence in aquatic environments. This work investigates the removal of MCPA (100 mg/L) in the aqueous phase via solar photo-Fenton. The process was carried out in a 700 mL reactor using a Xe lamp that simulates solar radiation (λ: 250–700 nm). A parametric study was conducted to assess the influence of dissolved O_2 on the reaction medium, Fe^{2+} dosage, H_2O_2 concentration and pH_0. The results indicate that dissolved O_2 boosts pollutant mineralization, even working at sub-stoichiometric H_2O_2 concentrations. Under optimal reaction conditions ($[Fe^{2+}]$: 7.5 mg/L, $[H_2O_2]_0$: 322 mg/L (stoichiometric dose), pH_0: 3.5), the MCPA reached almost complete mineralization (X_{TOC}: 98.40%) in 180 min. Phytotoxicity and ecotoxicity assessments of treated effluents revealed that even working at sub-stoichiometric H_2O_2 dosages, toxicity decreases with the solar photo-Fenton treatment. Finally, the solar photo-Fenton process was evaluated in relevant matrices (river water and WWTP secondary effluent) and a realistic pollutant concentration (100 μg/L). In all cases, the pollutant degradation was ≥70% in 60 min, demonstrating the potential of this technology as a tertiary treatment.

Keywords: advanced oxidation process; solar photo-Fenton; process intensification; water treatment; MCPA

check for updates

Academic Editors: Adolph Anga Muleja, Mukuna Patrick Mubiayi, Gcina Mamba, Adewale Adewuyi and Charmaine Sesethu Tshangana

Received: 15 June 2025
Revised: 4 July 2025
Accepted: 10 July 2025
Published: 15 July 2025

Citation: Martin-Montero, A.; Zapanti, A.M.; Pliego, G.; Casas, J.A.; Garcia-Costa, A.L. Solar Photo-Fenton: An Effective Method for MCPA Degradation. *Processes* **2025**, *13*, 2257. https://doi.org/10.3390/pr13072257

Copyright: © 2025 by the authors. Licensee MDPI, Basel, Switzerland. This article is an open access article distributed under the terms and conditions of the Creative Commons Attribution (CC BY) license (https://creativecommons.org/licenses/by/4.0/).

1. Introduction

The expansion of the agricultural sector to accommodate the increasing global population has inevitably led to the excessive application of pesticides and herbicides, subsequently contributing to the contamination of aquatic ecosystems [1,2]. This has placed substantial pressure on wastewater and drinking water treatment facilities, which must efficiently and rapidly eliminate pollutants such as 2-methyl-4-chlorophenoxyacetic acid (MCPA) [3,4]. In the 2023 monitoring campaign conducted by the Spanish Pesticide Risk Detection Network, MCPA was detected in groundwater samples at 5 out of 31 sampling points (17.2%). The mean concentration observed was 0.040 μg/L, with a maximum recorded value of 0.105 μg/L, slightly exceeding the standard threshold of 0.1 μg/L in one case [5]. This issue remains largely unresolved by conventional treatment methods, including commercial activated carbon filtration or incineration, which often fail to effectively remove certain pollutants from water sources [6]. In contrast, advanced oxidation processes (AOPs) emerge as promising alternatives for the degradation of these pollutants in water treatment [7,8]. AOPs rely in the generation of highly reactive species, such as hydroxyl

($HO^{\bullet}$), hydroperoxide ($HOO^{\bullet}$) or sulfate ($SO_4^{\bullet-}$) radicals, among others, to oxidize organic pollutants, aiming towards their complete mineralization.

Table 1 summarizes key studies that have employed AOPs for the degradation of MCPA in water. One of the processes investigated is ozonation, which utilizes gaseous ozone (O_3) in bubble contactor reactors [9]. This method has demonstrated a quick MCPA degradation (10 min). However, mineralization was not assessed, leaving the overall treatment efficacy uncertain. A comparative study was conducted on ozonation, UV, UV/H_2O_2 and O_3/H_2O_2 in MCPA degradation. It was demonstrated that advanced oxidation processes, namely, UV/H_2O_2 and O_3/H_2O_2 treatments, were more effective in degrading MCPA than individual ozonation or photolysis [10]. This suggests that the simultaneous generation of $HO^{\bullet}$ in these intensified processes substantially enhances the degradation efficiency of the contaminant. Similarly to the previous study, pollutant mineralization was not analyzed. Additionally, photocatalytic ozonation has been investigated as an alternative approach [11], as it combines the strong oxidative potential of ozone with the photocatalytic activity of B-TiO_2 as semiconductor material, leading to improved degradation kinetics compared to the use of TiO_2, reaching a total organic carbon (TOC) removal of 75%. Although ozonation is a well-established advanced oxidation process, it exhibits several limitations compared to alternative technologies. The limited solubility of ozone and its rapid decomposition in water significantly reduces its oxidative efficiency, particularly in complex matrices. Ozonation alone is often insufficient to meet water quality standards, necessitating additional treatment stages and thereby increasing both the operational complexity and overall cost.

Alternatively, sulfite was explored in the UV/sulfite system, aiming to generate highly reactive free radicals, including $SO_3^{\bullet-}$ and $HO^{\bullet}$. In this study, the herbicide was completely degraded, and full mineralization was achieved, leading to the generation of non-toxic reaction effluents [12]. Still, the addition of sulfite in the reaction medium leaves residual sulfate, which might compromise process feasibility. In contrast, H_2O_2-based processes offer a viable alternative, as their decomposition yields environmentally benign H_2O and O_2. In this scenario, the Fenton process is particularly noteworthy due to its high efficiency, the widespread availability of reagents and its relatively simple operational requirements. This process involves a redox cycle in an acidic medium, catalyzed by dissolved Fe^{2+}/Fe^{3+} [13]. Within this mechanism, H_2O_2 acts both as an oxidizing and reducing agent, generating $HO^{\bullet}$ and $HOO^{\bullet}$, as represented in Equations (1) and (2) [14]. These reactive species, characterized by their high oxidative potential (E_0 ($HO^{\bullet}$): +2.74 V; E_0 ($HOO^{\bullet}$): +1.70 V) [15], play a crucial role in in the degradation of organic matter.

$$Fe^{2+} + H_2O_2 \rightarrow HO^{\bullet} + OH^{-} + Fe^{3+} \qquad \left(k_{Fe^{2+}}:\ 40\text{–}80\ \mathrm{L/mol\ s}\right) \tag{1}$$

$$Fe^{3+} + H_2O_2 \rightarrow HOO^{\bullet} + H^{+} + Fe^{2+} \qquad \left(k_{Fe^{3+}}:\ 9.1 \times 10^{-7}\ \mathrm{L/mol\ s}\right) \tag{2}$$

The Fenton process is inherently limited by the regeneration rate of Fe^{2+}, as this reaction represents the slowest and thus, the rate-limiting step of the mechanism. To enhance the reaction kinetics, the technology can be intensified by applying UV-vis radiation, giving rise to the so-called photo-Fenton process. In this approach, light exposure accelerates the reduction of Fe^{3+} to Fe^{2+} (Equation (3)), thereby increasing the availability of the catalyst. Additionally, H_2O_2 photolysis (Equation (4)), which occurs at $\lambda < 380$ nm, contributes to the generation of $HO^{\bullet}$, further enhancing the system efficiency. As a result, UV-induced intensification of the Fenton process leads to higher reaction rates and improved pollutant degradation efficiency [16,17].

$$Fe^{3+} + H_2O + h\nu \rightarrow Fe^{2+} + HO^{\bullet} + H^{+} \tag{3}$$

$$H_2O_2 + h\nu \rightarrow 2\,HO^{\bullet} \quad (4)$$

The Fenton process was applied to the treatment of MCPA, achieving over 90% degradation of the pollutant [18]. However, no data on mineralization were reported, despite this being the only study to perform a test with low contaminant concentrations and surface water as a relevant aqueous matrix. In contrast, the photoelectron-Fenton process was employed, where hydrogen peroxide was generated at the cathode and, combined with UV radiation, resulted in the complete mineralization of the contaminant [19].

Although UV-assisted Fenton processes are effective, their high energy requirements raise concerns about techno-economic viability, primarily due to electricity consumption compared to conventional biological treatments [20]. In response, growing research has focused on solar-driven photocatalytic processes [21–23], which leverage solar radiation as a renewable, abundant and environmentally benign energy source. This approach offers a sustainable and economically favorable alternative by significantly reducing dependence on conventional electricity sources [24].

Although previous studies have investigated MCPA degradation using various advanced oxidation processes (AOPs), important gaps remain. In particular, most works have focused on degradation efficiency under ideal conditions, overlooking key aspects such as the extent of pollutant mineralization, the reduction in toxicological effects and the overall process feasibility in real-world applications. These gaps are especially evident when AOPs are tested at environmentally relevant concentrations and in complex matrices, as summarized in Table 1. Moreover, few studies have explored alternatives to conventional UV-based systems in terms of energy efficiency and operational costs.

Therefore, this work tackles these critical issues by proposing solar photo-Fenton as a cost-effective and sustainable alternative to UV-assisted systems [25]. The study not only optimizes treatment conditions but also evaluates performance in terms of mineralization and toxicity reduction, using environmentally relevant matrices such as river water and secondary effluent from a wastewater treatment plant. In doing so, this work addresses several underexplored aspects that are essential for the real-world application of AOPs.

Table 1. Degradation of MCPA with AOPs.

AOP	Catalyst	Operating Conditions	Results	Observations	Reference
Ozonation	-	$[MCPA]_0$: 80 mg/L, T: 20 °C, Q_g: 0.06 m^3/h, $[TBA]_0$: 5 mM	X_{MCPA}: 100%	Experiments were conducted in the presence of tert-BuOH as hydroxyl scavenger.	[9]
UV/H_2O_2	-	$[MCPA]_0$: 50 mg/L, $[H_2O_2]_0$: 68 mg/L, T: 20 °C	X_{MCPA}: 100%	Synergic effects of O_3 and hydroxyl radicals.	[10]
O_3/H_2O_2	-		X_{MCPA}: 100%		
Photocatalytic ozonation	B-doped TiO_2	$[MCPA]_0$: 5 mg/L, [cat]: 0.33 g/L, $[O_{3\ g\ inlet}]$: 5 mg/L pH_0: 6.5, T: 25–40 °C, t: 120 min	X_{MCPA}: 100% X_{TOC}: 75%	The catalytic activity was maintained after 3 consecutive runs with no boron leaching detected.	[11]
UV/Sulfite reduction	-	$[MCPA]_0$: 50–200 mg/L MCPA:Sulfite ratio 3:1, pH_0: 11, t: 30 min	X_{MCPA}: 100% X_{TOC}: 100%	Effluent toxicity: very low after treatment (Kirby-Bauer disc method).	[12]
Fenton	Fe^{2+}	$[MCPA]_0$: 10 mg/L and 1.5 µg/L, Fe (II): 2.5 mg/L, H_2O_2: 1.53 mg/L, pH_0: 3–6.5, t: 120 min	X_{MCPA}: >90%	Study in relevant pollutant concentrations (1.5 µg/L) and surface water.	[18]
Electro-Fenton	Fe^{2+}	$[MCPA]_0$: 380 mg/L, $[Fe^{2+}]$: 5 mg/L, pH_0: 3, T: 35 °C, t: 360 min	X_{MCPA}: 100% X_{TOC}: 70–75%	H_2O_2 electrogenerated on the cathode.	[19]

2. Materials and Methods

2.1. Reactants

2-methyl-4-chlorophenoxyacetic acid (MCPA, 98 wt%, CAS No.: 5221-16-9), provided by Sigma Aldrich (Darmstadt, Germany), was used as the model pollutant for the degradation experiments. Hydrogen peroxide (H_2O_2, 30% v., CAS No.: 7722-84-1) provided by Merck (Darmstadt, Germany) was employed as the oxidant agent. Iron (II) chloride tetrahydrate ($FeCl_2 \cdot 4H_2O$, ≥99 wt%, CAS No.: 13478-10-9) provided by Sigma-Aldrich (Darmstadt, Germany), served as the catalyst. Sulfuric acid (H_2SO_4, 96–98% v., CAS No.: 7664-93-9), sodium bicarbonate ($NaHCO_3$, ≥99 wt%, CAS No.: 144-55-8), sodium carbonate (Na_2CO_3, ≥99 wt%, CAS No.: 497-19-8), acetonitrile (HPLC grade, CAS No.: 75-05-8), formic acid (HCOOH, 98% v., CAS No.: 64-18-6) and titanium (IV) oxysulfate (1.9–2.1% v., CAS No.: 13825-74-6), all supplied by Panreac (Barcelona, Spain), were employed in the analytical procedures. All the reagents were used without further purification. Ultrapure water, generated using an Autwomatic Plus 1+2 GR system (Wasserlab, Navarra, Spain), was utilized throughout the work.

2.2. Typical Procedure for Oxidation Experiments

The oxidation experiments were conducted in a jacketed immersion-wall batch photoreactor that simulates solar radiation, with a capacity of 700 mL. The system was equipped with a 180 W xenon lamp (T-Xe, Heraeus, Hanau, Germany) enclosed within a water-cooled quartz chamber and integrated with a temperature control unit, ensuring the reaction temperature was maintained at 25 °C (Ministat 125, Huber, Atlanta, GA, USA). The lamp emitted across a broad spectrum ranging from 250 to 700 nm, λ_{max} = 467 nm (Figure A1 of Appendix A), with a UV-C irradiance of 120 W/m^2, UV-A irradiance of 1250 W/m^2 and visible irradiance of 596 W/m^2, as measured by a photoradiometer (Delta Ohm, model 2102.1, Padua, Italy). The photoreactor was positioned on a stirring plate (IKA RCT Basic, Wilmington, DC, USA) and operated under magnetic stirring at 550 rpm under ambient conditions. These conditions were applied throughout the work.

The MCPA degradation was first studied by means of photolysis (UV), UV/H_2O_2, dark Fenton and solar photo-Fenton working at 100 mg/L MCPA, 5 mg/L Fe^{2+} and 322 mg/L H_2O_2, which corresponds to the stoichiometric dose required for complete mineralization. Photolysis (UV) refers to the direct irradiation of the solution with ultraviolet light in the absence of any added reagents, aiming to assess the degradation of MCPA by direct photochemical pathways. The UV/H_2O_2 process combines UV light with hydrogen peroxide to generate hydroxyl radicals through photolytic cleavage of H_2O_2, enhancing oxidative degradation. The dark Fenton process involves the reaction between Fe^{2+} and H_2O_2 in the absence of light, producing hydroxyl radicals via Fenton chemistry under dark conditions. Lastly, the solar photo-Fenton process incorporates both Fe^{2+} and H_2O_2 under solar irradiation, promoting additional radical generation through the photo-reduction of Fe^{3+} and photolysis of H_2O_2, thus intensifying the oxidative capacity of the system. These four processes were evaluated under identical initial conditions in order to compare their efficiency in degrading the MCPA and to understand the contribution of each individual mechanism to the overall removal and potential mineralization of the pollutant.

After evaluating the different processes, a parametric study of the solar photo-Fenton system was performed to investigate the influence of key operational parameters. In each case, a single parameter was varied while keeping the others constant, based on the conditions established in the initial experiment, in the first section. To verify the influence of the dissolved O_2 in the reaction, the photo-Fenton experiment shown in the first section was repeated under inert conditions, with constant N_2 bubbling at Q_{N2}: 50 mLN/min. To assess the effect of catalyst concentration on the photo-Fenton process, Fe^{2+} concentration

was varied between 1.5 and 7.5 mg/L. The MCPA degradation was also investigated by varying the H_2O_2 concentration within the range of 25–100% relative to the stoichiometric amount required for complete mineralization. Given that photo-assisted processes might allow a larger operational window regarding pH_0, the process was evaluated within a pH_0 range of 3.5 to 6 to assess its feasibility at circumneutral pH.

The effluents obtained from the experiments evaluating different H_2O_2 dosages were analyzed by ion chromatography to identify and quantify the short-chain organic acids generated as potential oxidation byproducts. In addition, these effluents were subjected to phytotoxicity and ecotoxicity assays to evaluate the potential environmental impact of the residual compounds present after treatment. The procedures for the toxicity assays are described in detail in a subsequent section.

To evaluate the influence of the water matrix on the efficiency of the solar photo-Fenton process, two representative environmental matrices were selected: river water from Lastras de Cuéllar (Segovia, Spain) and secondary effluent from a wastewater treatment plant (WWTP) located in Madrid (Spain). These samples were collected, filtered through 0.45 µm nylon membranes and fully characterized to assess their physicochemical composition. Detailed characterization of both matrices is presented in Table A1 of Appendix A. As shown, the river water exhibited very low concentrations of organic carbon, with a notable presence of inorganic carbon species such as carbonate (CO_3^{2-}), bicarbonate (HCO_3^-) and nitrate (NO_3^-). In contrast, the WWTP effluent showed significantly higher levels of total organic carbon (TOC), as well as chloride (Cl^-), nitrate (NO_3^-) and sulfate (SO_4^{2-}). Before carrying out the experiments, both matrices were spiked with 100 µg/L of MCPA and acidified to an initial pH of 3.5 to ensure comparability with the results obtained in ultrapure water. In this case, an amount of iron corresponding to 1 mg/L and a hydrogen peroxide dose of 10 mg/L were used for this section.

The MCPA evolution was adequately described by a pseudo-first-order kinetic model, as shown in Equation (5).

$$\frac{d\,[MCPA]}{dt} = -k_{app}\cdot[\mathrm{MCPA}] \quad (5)$$

2.3. Analytical Methods

Samples were periodically collected from the reactor, filtered through 0.45 µm nylon filters (Scharlau) and immediately analyzed. The identification and quantification of the MCPA were performed using an Ultra HPLC system (Thermo Scientific Ultimate 3000, Waltham, MA, USA) with a Diode Array Detector (Dionex Ultimate 3000, Waltham, MA, USA). The mobile phase comprised a binary mixture (60:40) of water and acetonitrile, both acidified with 0.1% formic acid, delivered at a flow rate of 0.75 mL/min under isocratic conditions. The stationary phase was a ZORBAX Eclipse Plus C18 column (100 mm, 1.8 µm). The detection of the MCPA was achieved with a UV detector set to a wavelength of 229 nm. The reaction intermediates and water matrices characterization were evaluated with an ionic chromatographer (Methrom 790 IC, Herisau, Switzerland) with chemical suppression and a conductivity detector. The stationary phase consisted of a Metrosep A Supp 5–20 column (25 cm × 4 mm), while the mobile phase used a 3.2 mM/1 mM aqueous solution of Na_2CO_3 and $NaHCO_3$, respectively, carried at a flow rate of 0.7 mL/min. The total organic carbon (TOC) was determined using a TOC analyzer (Shimadzu TOC-VSCH, Kyoto, Japan). The residual H_2O_2 present in the liquid phase was quantified through colorimetric titration, employing the $TiOSO_4$ method [26] and an Agilent spectrophotometer.

2.4. Toxicity Assessment

Phytotoxicity assessments were conducted using standardized phytotoxicity tests kits (Phytotestkit microbiotest; MicroBioTest Inc., Ghent, Belgium), in accordance with ISO

Standard 1876 (2016) [27]. These assays evaluated the seed germination and early growth in three plant species (*Sinapsis Alba*, *Lepidium sativum*, *Sorghum saccharatum*), incubated at 25 °C for 72 h. Following incubation, the germination rates were determined for both the untreated samples and treated effluent, after pH adjustment to a range of 6–8. Additionally, the root and shoot lengths were measured. ImageJ software was employed for the data analysis, and the relative growth was calculated using Equation (6).

$$\% \text{ relative growth} = \frac{L_T - L_{NT}}{L_T} \cdot 100 \quad (6)$$

where L_T represents the root and shoots length in the treated samples and L_{NT} corresponds to the root and shoot length in the initial (non-treated) samples.

We used the Microtox protocol (ISO 11348-3, 1998) [28], utilizing an M500 Microtox Analyzer (Azur Environmental, Egham, UK) at 15 °C. Prior to the assay, the pH of the samples was adjusted to a range of 6–8, and salinity was set to 2% NaCl. The EC_{50} value serves as a measure of ecotoxicity, indicating the nominal concentration (mg/L) of the substance required to reduce bioluminescence by 50% after 15 min exposure [29]. In the case of complex samples, the IC_{50} is used instead, representing the dilution ratio at which the same 50% reduction occurs. Both the EC_{50} and IC_{50} values exhibit an inverse relationship with biological toxicity, which is expressed in toxicity units. This relationship is mathematically defined by Equation (7), where C_0 denotes the initial compound concentration used to determine the EC_{50} value [30].

$$TU = \frac{C_0 \left(\frac{mg}{L}\right)}{EC_{50} \left(\frac{mg}{L}\right)} = \frac{100}{IC_{50}} \quad (7)$$

3. Results and Discussion

3.1. Process Evaluation for MCPA Oxidation

The results, presented in Figure 1, show that the MCPA exhibits photostability, implying that the employed solar simulation lamp does not induce significant degradation of MCPA during the reaction. The UV/H_2O_2 process resulted in a slow degradation of the MCPA and H_2O_2 consumption. These results agree with reports in the literature, which indicate that more energetic UV radiation, within the UV-C range (λ = 100–280 nm), is necessary to achieve the homolytic cleavage of H_2O_2, leading to the generation of $HO^{\bullet}$ [31]. The incorporation of Fe^{2+} as the catalyst in the Fenton process significantly enhances the MCPA removal while promoting peroxide decomposition, leading to a 25% mineralization rate, as illustrated in Figure A2 of Appendix A. Notably, the catalytic activity of Fe^{2+} can be further enhanced using solar radiation, achieving total MCPA elimination in 30 min and complete H_2O_2 decomposition, with a 98.5% mineralization degree, at t: 180 min.

The kinetic results for the MCPA degradation, shown in Table 2, clearly demonstrate that the solar photo-Fenton process was by far the most efficient, achieving the highest apparent reaction rate constant. This was followed by the dark Fenton process, which was also significantly faster than UV/H_2O_2 and photolysis, as expected. This hierarchy highlights the superior performance of Fenton-based processes, especially when intensified with solar radiation.

Kinetic data from UV, UV/H_2O_2, dark Fenton (H_2O_2/Fe^{2+}) and photo-Fenton (UV/H_2O_2/Fe^{2+}) were utilized to calculate the process synergy factor, as defined in Equation (8). A synergy factor exceeding 1 indicates an enhancement of reaction kinetics due to the process integration. Under the studied conditions, the synergy factor for the MCPA degradation in the solar photo-Fenton process was determined to be f_{syn}:

9.05, demonstrating a substantial improvement due to the synergic mechanisms in the solar-intensified process.

$$f_{syn} = \frac{k_{app,photoFenton}}{k_{app,Photolysis} + k_{app,UV/H_2O_2} + k_{app,Fenton}} \quad (8)$$

Table 2. Apparent kinetic constants for MCPA degradation.

Process	$k_{app,MCPA}$ (min^{-1})	r^2
Photolysis	9.90×10^{-4}	0.967
UV/H_2O_2	2.42×10^{-3}	0.983
Dark Fenton	1.20×10^{-2}	0.949
Photo-Fenton	1.39×10^{-1}	0.986

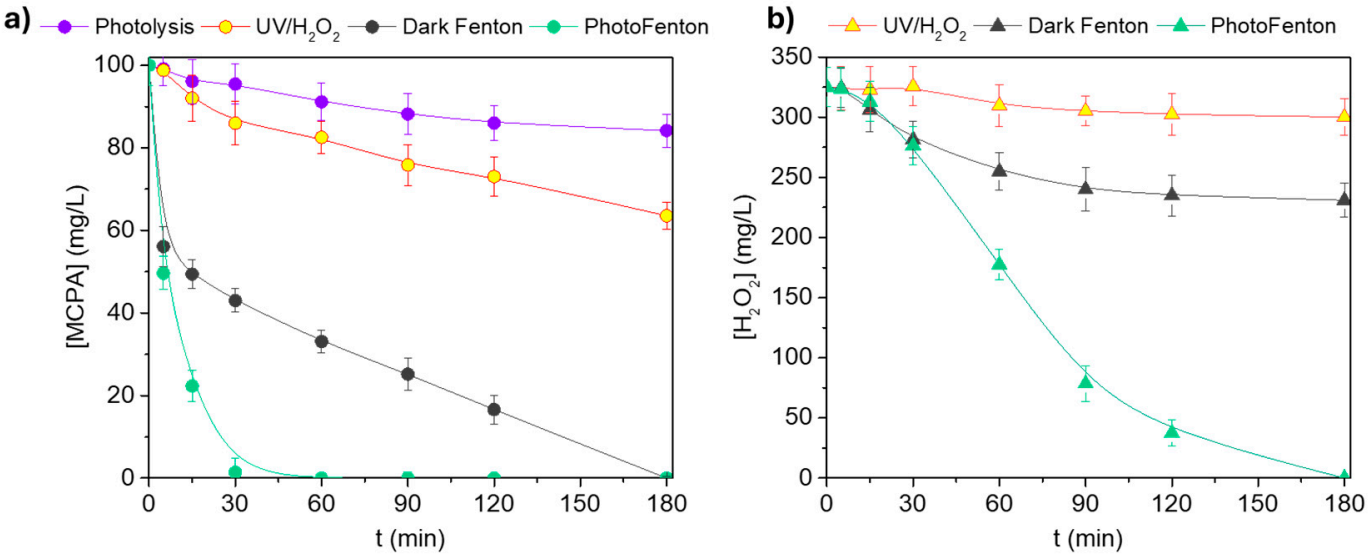


Figure 1. (**a**) MCPA degradation and (**b**) H_2O_2 consumption for the studied processes. Operating conditions: $[MCPA]_0$: 100 mg/L, $[H_2O_2]_0$: 322 mg/L (100% stoichiometric), $[Fe^{2+}]$: 7.5 mg/L, pH_0: 3.5, T: 25 °C.

3.2. Parametric Study

3.2.1. Effect of Dissolved O_2

Figure 2a illustrates that the degradation of the MCPA proceeds slightly faster in presence of O_2. Analyzing Figure 2b, which represents H_2O_2 exploitation, the diagonal represents the ideal behavior of the photo-Fenton process operating at the stoichiometric oxidant dose, where each fraction of converted H_2O_2 corresponds to the elimination of an equivalent fraction of TOC [32]. Notably, in the presence of O_2, at 10% H_2O_2 conversion, the degree of mineralization exceeds the predicted value, reaching X_{TOC}: 50%. This deviation is attributed to the role of the dissolved O_2, which can react with organic radicals to generate $HOO^{\bullet}$, as illustrated in Equations (9) and (10) [33]. A similar phenomenon has been reported in the degradation of cyclohexanecaboxylic acid in a UV-A-assisted photo-Fenton process [32].

$$R^{\bullet} + O_2 \rightarrow RO_2^{\bullet} \quad (9)$$

$$RO_2^{\bullet} + H_2O_2 \rightarrow CO_2 + R'H + HOO^{\bullet} \quad (10)$$

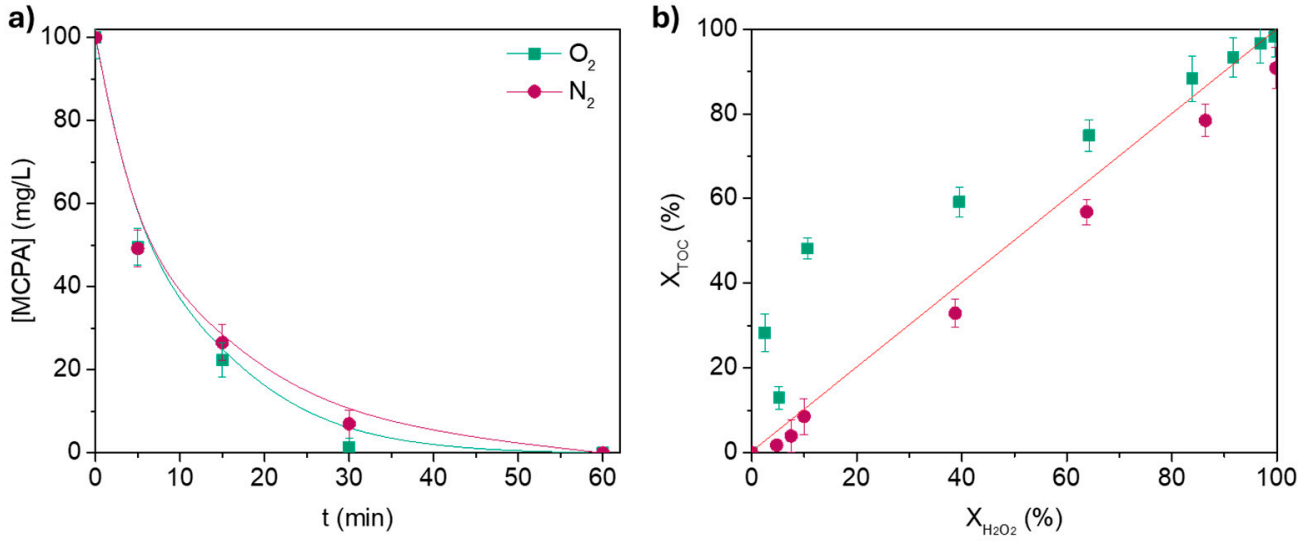


Figure 2. (**a**) MCPA degradation and (**b**) H_2O_2 exploitation. Operating conditions: $[MCPA]_0$: 100 mg/L, $[H_2O_2]_0$: 322 mg/L (100% stoichiometric), $[Fe^{2+}]$: 7.5 mg/L, pH_0: 3.5, T: 25 °C.

Consequently, subsequent experiments were conducted in the presence of O_2 to achieve higher rates of pollutant mineralization.

3.2.2. Catalyst Concentration

The results for MCPA degradation and H_2O_2 consumption are depicted in Figure 3. As expected, increasing the catalyst concentration enhances the rate of MCPA removal, as evidenced in Figure 3a and corroborated by the kinetic data shown in Table 3. Similarly, Figure 3b shows that the rate of peroxide consumption is also boosted when the catalyst concentration is increased, as more Fe^{2+} means a faster iron regeneration cycle, which allows the reaction to be maintained and accelerated [34].

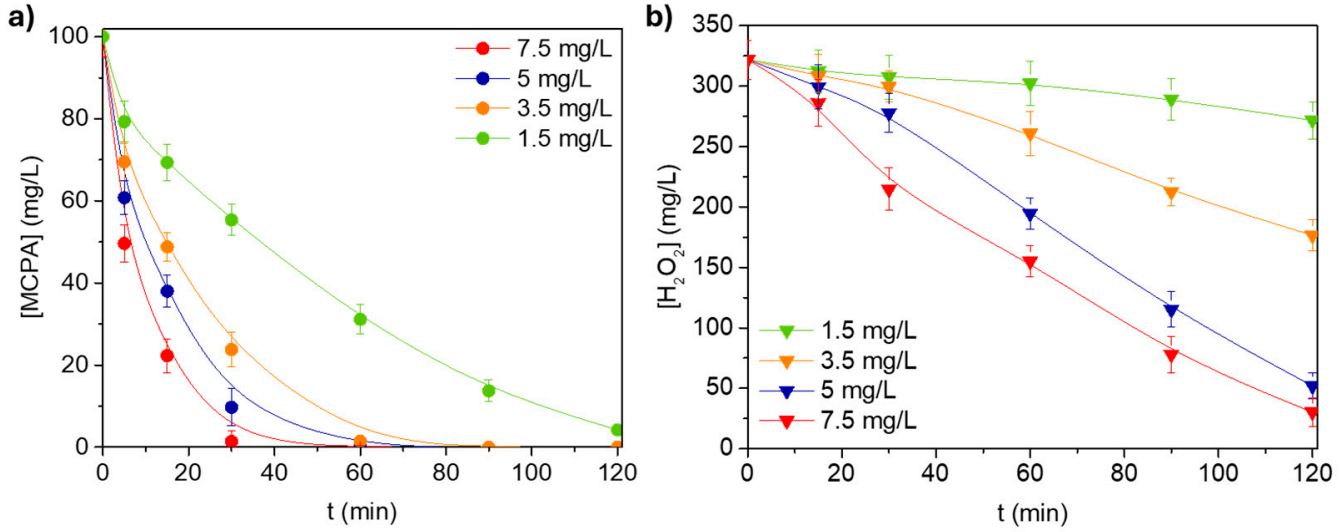


Figure 3. Influence of Fe^{2+} load on (**a**) MCPA degradation and (**b**) H_2O_2 consumption. Operating conditions: $[MCPA]_0$: 100 mg/L, $[H_2O_2]_0$: 322 mg/L (100% stoichiometric), pH_0: 3.5, T: 25 °C, t: 120 min.

Table 3. Apparent kinetic rate constants and specific rate constants for MCPA degradation in the catalyst load study.

$[Fe^{2+}]$ (mg/L)	$k_{app,MCPA}$ (min^{-1})	$k_{spc,MCPA}$ ($L/min \cdot g_{cat}$)	r^2
1.5	2.50×10^{-2}	16.40	0.987
3.5	6.90×10^{-2}	18.30	0.984
5	9.20×10^{-2}	18.40	0.985
7.5	13.97×10^{-2}	18.60	0.986

The kinetic analysis results indicate that increasing the Fe^{2+} concentration from 1.5 to 7.5 mg/L significantly catalyzes the reaction, evidenced by a notable increase in the apparent rate constant ($k_{app,MCPA}$). Although the specific rate constant ($k_{spc,MCPA}$), defined as the apparent kinetic constant normalized by the catalyst concentration employed, also showed a slight initial increase, it tended to stabilize at higher Fe^{2+} concentrations, suggesting that potential limitations by other factors such as Fe^{2+} availability become less restrictive. At all the tested catalyst concentrations, complete MCPA degradation was achieved within 120 min of reaction. However, higher catalyst concentrations resulted in higher mineralization rates, as can be seen in Figure A3. In addition, a linear relationship was found between the concentration of iron used and the apparent kinetic constant, as shown in Figure A4.

Accordingly, this Fe^{2+} dosage (7.5 mg/L) was selected for further experimental investigations.

3.2.3. H_2O_2 Dosage

The primary operational expense associated with the Fenton process is H_2O_2 consumption [35]. Therefore, optimizing H_2O_2 usage is essential for developing cost-effective water treatment technologies. The results for the MCPA evolution along the reaction, presented in Figure 4a, show that the MCPA conversion was complete after 60 min of reaction in all the evaluated cases. The experimental results demonstrate that the H_2O_2 dosage is a determining factor in the kinetics of the MCPA degradation process, shown in Table 4. An increase in the H_2O_2 dosage from 25% to 100% resulted in a significant increase in the apparent rate constant ($k_{app,MCPA}$), which rose from 7.74 to 13.97 min^{-1}. Similarly, the mineralization rate also improved with higher dosages of H_2O_2, as seen in Figure 4b, again showing a linear relationship between the apparent kinetic constant and the H_2O_2 dosage (Figure A5). Although all the sub-stoichiometric H_2O_2 dosages led to a higher mineralization rate than expected due to the role of the dissolved O_2, complete mineralization was not reached. Hence, using lower oxidant doses, there is an incomplete MCPA degradation, which could indicate the presence of harmful intermediates, such as chlorinated byproducts that might exhibit greater toxicity than the parent compound, as observed in the case of the Fenton oxidation of chlorophenols [36].

Table 4. Apparent kinetic rate constants and specific rate constants for MCPA degradation in the H_2O_2 dose study.

H_2O_2 Dose	$k_{app,MCPA}$ (min^{-1})	r^2
25%	7.74×10^{-2}	0.987
50%	9.77×10^{-2}	0.982
75%	11.45×10^{-2}	0.992
100%	13.97×10^{-2}	0.972

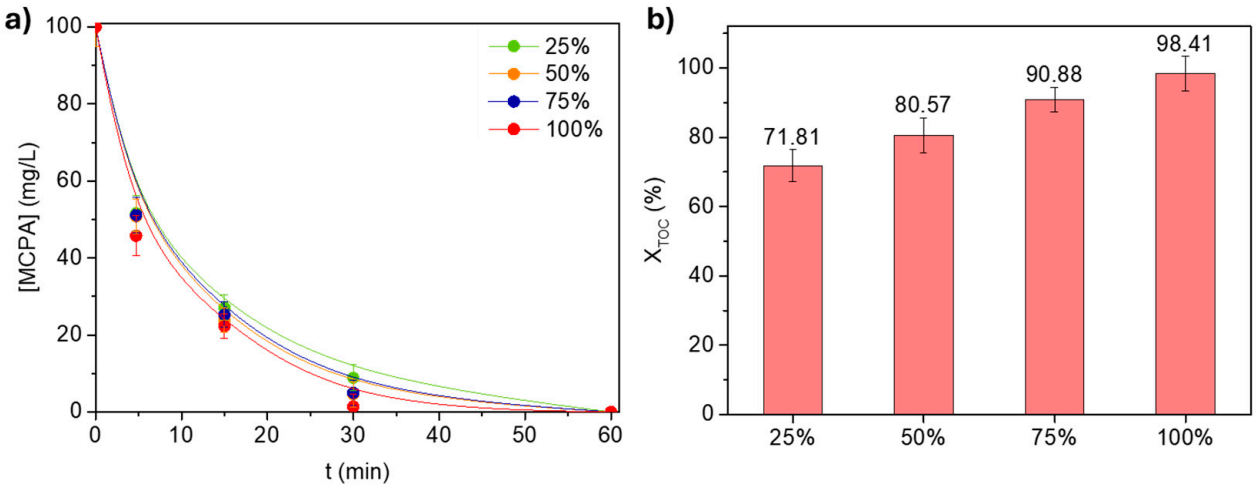


Figure 4. Influence of H_2O_2 dosage on (**a**) MCPA degradation and (**b**) mineralization degree. Operating conditions: $[MCPA]_0$: 100 mg/L, $[Fe^{2+}]$: 7.5 mg/L, pH_0: 3.5, T: 25 °C.

Thus, to ensure maximized pollutant depletion, the stoichiometric H_2O_2 dosage (H_2O_2: 322 mg/L) was chosen for the subsequent experimental assays.

3.2.4. pH_0

Another limitation in homogenous Fenton processes is the operational pH. Homogeneous Fenton, employing Fe^{2+} as a catalyst, operates effectively only within a narrow pH range between 2.5–3.5. The Fe^{3+} ions formed during the reaction begin to precipitate as ferric hydroxide ($Fe(OH)_3$) or as iron oxyhydroxides, such as FeO(OH), when increasing the pH. This precipitation reduces the concentration of dissolved iron, slowing down the continuation of the catalytic cycle and the production of $HO^{\bullet}$ [37,38]. However, in the photo-Fenton process, when the $Fe(OH)^{2+}$ complex absorbs a photon (hν), a ligand-to-metal charge transfer (LMCT) reaction occurs, leading to its decomposition and the generation of Fe^{2+} and a hydroxyl radical ($HO^{\bullet}$) (Equation (11)) [39].

$$Fe(OH)^{2+} + h\nu \rightarrow Fe^{2+} + HO^{\bullet} \quad (11)$$

The results for MCPA evolution and H_2O_2 consumption are shown in Figure 5. Both graphs reveal a marked pH dependence, with optimal efficiency observed at pH_0 3.5. Under this operating condition, the MCPA degradation is the fastest, as shown in Table 5, and the H_2O_2 consumption is also the most efficient, indicating optimal $HO^{\bullet}$ generation. Conversely, as the pH_0 increases towards values of 5 and 6, both the MCPA degradation and H_2O_2 consumption slow down drastically, highlighting the significant reduction in the kinetics of the photo-Fenton process under less acidic conditions, primarily due to the limited availability of dissolved iron. Nonetheless, practically complete MCPA degradation is reached after 90 min in all cases. Figure A5 shows the extent of the mineralization achieved under the tested conditions. Although the process progresses more slowly at near-neutral pH, the final mineralization levels are comparable. The stability of the mineralization across pH values suggests that, despite the reduced reaction rates, the effective degradation of MCPA and effective H_2O_2 consumption can still be achieved at circumneutral pH. This allows the process to operate within a broader and more practical pH range without compromising treatment performance.

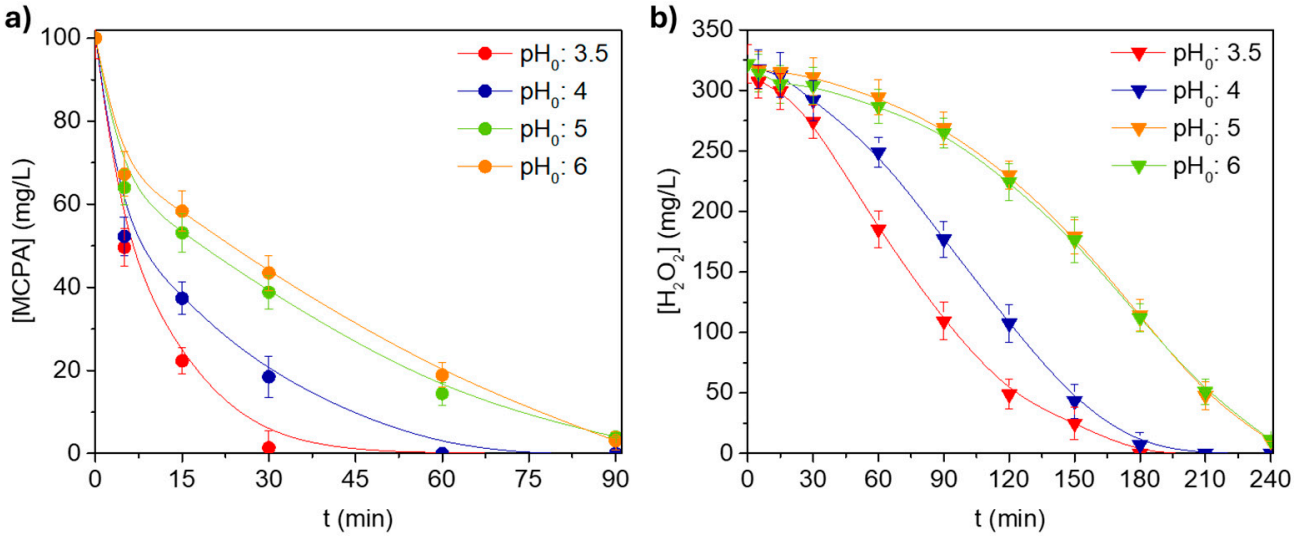


Figure 5. Influence of pH_0 on (**a**) MCPA degradation and (**b**) H_2O_2 consumption in solar photo-Fenton. Operational conditions: $[MCPA]_0$: 100 mg/L, $[Fe^{2+}]$: 7.5 mg/L, $[H_2O_2]_0$: 322 mg/L (100% stoichiometric), T: 25 °C.

Table 5. Apparent kinetic rate constants and specific rate constants for MCPA degradation in the pH_0 study.

pH_0	$k_{app,MCPA}$ (min^{-1})	r^2
3.5	13.97×10^{-2}	0.972
4	5.17×10^{-2}	0.950
5	3.78×10^{-2}	0.985
6	3.35×10^{-2}	0.953

In summary, the parametric study indicates that the optimal conditions for the solar photo-Fenton treatment of MCPA-contaminated water include a catalyst concentration of 7.5 mg/L, a hydrogen peroxide dosage at its stoichiometric ratio and pH_0: 3.5–5, in the presence of dissolved O_2.

3.3. Reaction Intermediates and Toxicity Assessment

In Section 3.2.3, the use of sub-stoichiometric H_2O_2 dosages limited the pollutant mineralization, which implies the presence of reaction byproducts that could possess a high toxicity [36]. The primary byproducts identified were chloride and formic, acetic, maleic, malonic, fumaric and oxalic acids. The carbon balance corresponding to these byproducts is depicted in Figure 6 as calculated TOC and compared to the measured TOC. At low H_2O_2 dosages (25 and 50%), there is a large difference between the measured and the calculated TOC, indicating the presence of unidentified reaction byproducts. In contrast, working at higher H_2O_2 concentrations, there is a greater match between the measured and the calculated TOC, with the total carbon content being primarily attributed to these organic acids. This suggests that these effluents are readily biodegradable and potentially non-toxic. Additionally, analysis of the released chloride, shown in Figure 6b, corroborates that the said non-identified reaction intermediates correspond to chlorinated compounds. Hence, toxicity analyses must be performed to assess the viability of this process.

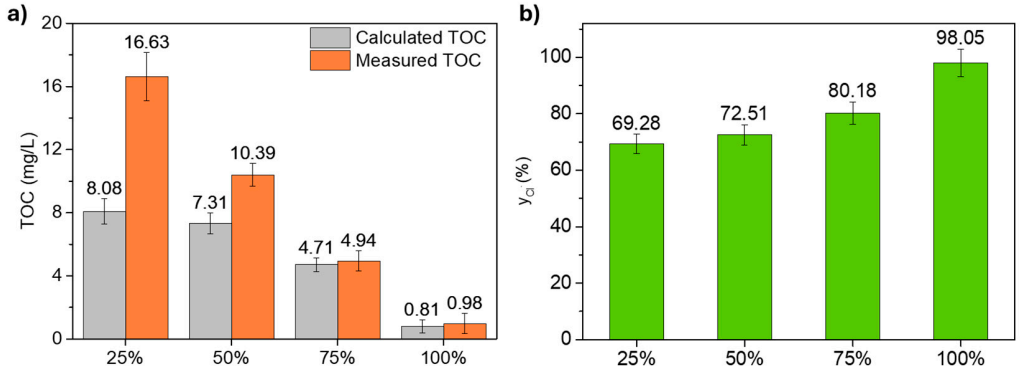


Figure 6. (**a**) Carbon balance in final effluents varying the H_2O_2 stoichiometric dose, (**b**) chloride release into the medium. Operating conditions: $[MCPA]_0$: 100 mg/L, $[Fe^{2+}]$: 7.5 mg/L, pH_0: 3.5, T: 25 °C.

In order to verify the toxicity of the effluents resulting from these treatments, qualitative phytotoxicity and quantitative ecotoxicity tests were conducted. These assays aimed to evaluate the potential environmental impact of the treated water, particularly considering the presence of unidentified reaction intermediates, which may still contribute to residual toxicity [36]. Figure 7 presents the results of the phytotoxicity tests in relation to the H_2O_2 dosage employed. The relative growth of stems and roots was obtained by comparing seeds watered with the effluents to seeds watered with the influent, containing 100 mg/L MCPA. The results indicate that the treated effluents exhibited lower toxicity than the initial solution, further reinforcing the feasibility of this process for MCPA degradation and the reduction in its associated toxicity. However, it is important to note that, as expected, the decrease in toxicity was less pronounced when applying 25 and 50% of the stoichiometric dose of the oxidizing agent compared to 75 and 100%.

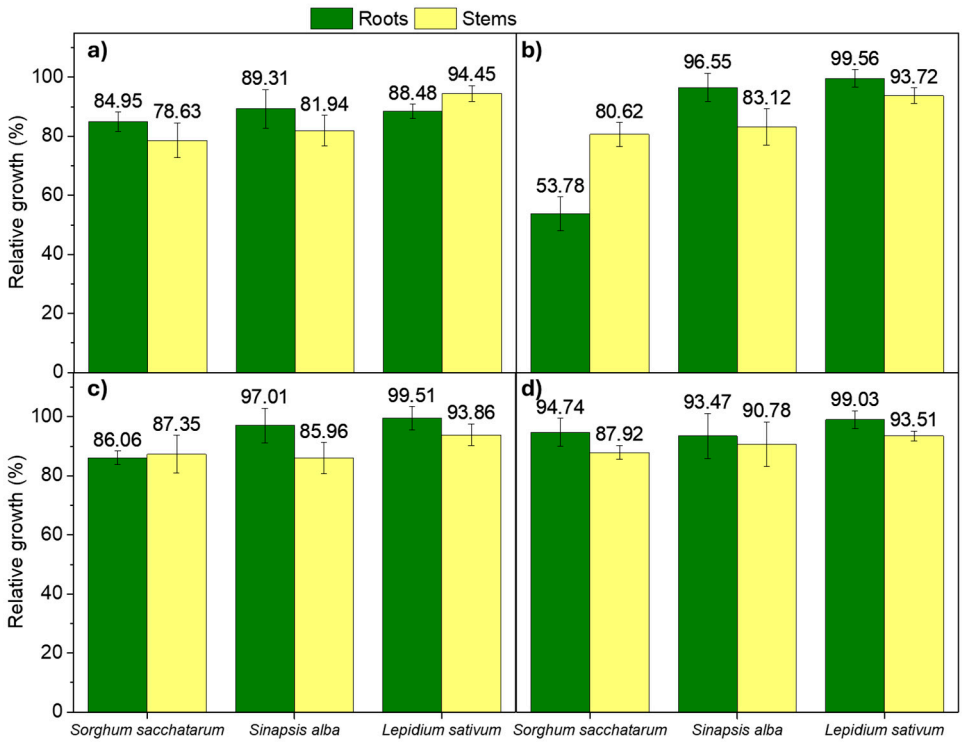


Figure 7. Phytotoxicity test for solar photo-Fenton for (**a**) 25% (**b**) 50% (**c**) 75% and (**d**) 100% of H_2O_2 stoichiometric dosage. Operating conditions: $[MCPA]_0$: 100 mg/L, $[Fe^{2+}]$: 7.5 mg/L, pH_0: 3.5, T: 25 °C, t: 120 min, ultrapure water.

To gain further knowledge on the toxicity of the effluents, ecotoxicity runs were performed using *Aliivibrio fischeri* bioassays. The results, presented in terms of toxicity units (TUs) after a 15 min exposure (Figure 8), reveal a significant decrease in the effluents' ecotoxicity. According to the literature [40], effluents are categorized based on TU values as negligibly toxic (TU < 1), toxic (TU: 1–10), very toxic (TU: 11–100) and extremely toxic (TU > 100). Following this classification, the initial solution containing 100 mg/L of MCPA was classified as very toxic. A significant reduction in toxicity was observed when higher doses of oxidant were applied. As expected, the highest level of detoxification was achieved with the use of a stoichiometric dose of H_2O_2, resulting in a non-toxic effluent. In contrast, the sub-stoichiometric doses used (50 and 75%) produced slightly toxic effluents approaching the toxicity threshold defined in the literature. Finally, a slight reduction in the ecotoxicity of the effluent treated with 25% of the stoichiometric amount is observed; however, it remains within the range of toxic substances. Short-chain organic acids are relatively biodegradable and exhibit low individual toxicity. Hence, their presence at the levels detected in this study is unlikely to account for the observed ecotoxicity and phytotoxicity in the treated effluents. Therefore, the residual toxicity observed when using 25% and 50% H_2O_2 dosages is more likely attributable to the formation of unidentified transformation products, as shown in Figure 6a. This suggests that the unidentified reaction intermediates manifest toxic properties, even though they are less toxic than MCPA.

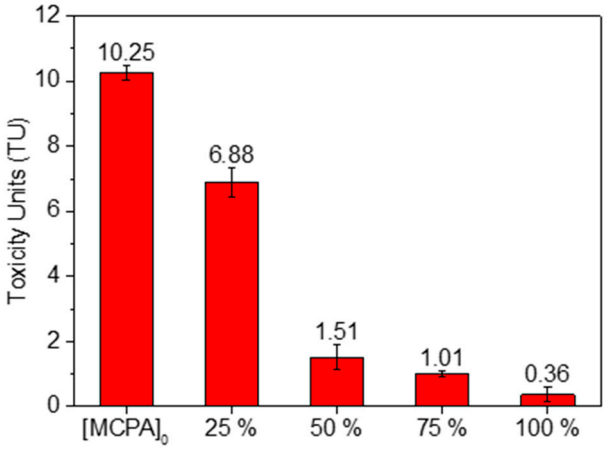


Figure 8. Ecotoxicity results for *Aliivibrio fischeri* in toxicity units for the different hydrogen peroxide doses. Operating conditions: $[MCPA]_0$: 100 mg/L, $[Fe^{2+}]$: 7.5 mg/L, pH_0: 3.5, T: 25 °C, t: 120 min, ultrapure water.

3.4. Water Matrices Assessment

The characteristics of the water matrix significantly influence oxidation processes [41–43]. Consequently, evaluating the applicability of the solar photo-Fenton process for MCPA degradation in water matrices of greater complexity than ultrapure water is essential. WWTP water and river water exhibit a complex composition, characterized by higher organic matter load and inorganic species concentration. The results for the MCPA removal, presented in Figure 9, indicate that as the complexity of the water matrix increases, the MCPA degradation slows down. In the river water, the presence of inorganic carbon, specifically carbonate, acts as a hydroxyl radical scavenger, via the generation of carbonate radical ($CO_3^{\bullet-}$), as shown in Equation (12). $CO_3^{\bullet-}$ possesses a lower oxidation potential (E_0 ($CO_3^{\bullet-}$): +1.8 V) and a lower reactivity than $HO^{\bullet}$, which reduces the oxidation efficiency [44,45].

$$HO^{\bullet} + CO_3^{2-} \rightarrow CO_3^{\bullet-} + OH^{-} \quad (12)$$

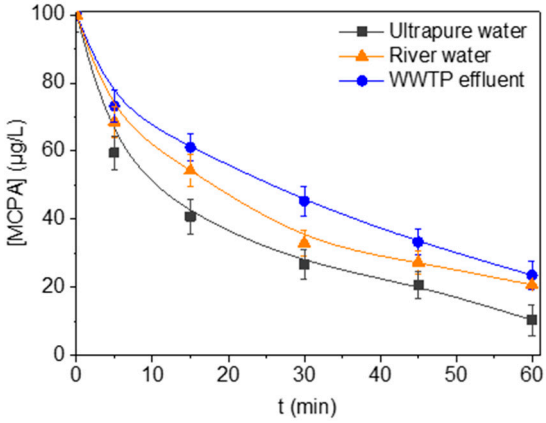


Figure 9. MCPA evolution under solar photo-Fenton in ultrapure water, river water and secondary WWTP effluent. Operating conditions: $[MCPA]_0$: 100 µg/L, $[H_2O_2]_0$: 10 mg/L, $[Fe^{2+}]$: 1 mg/L, pH_0: 3.5, T: 25 °C.

However, the most influencing parameter regarding process efficiency is the organic matter content (TOC), which can be overcome by adapting the H_2O_2 dosage in complex matrices by calculating the stoichiometric H_2O_2 dose in relation to the Chemical Oxygen Demand (COD). Strong competition between natural organic matter and MCPA for reactive radicals leads to a decreased degradation rate in the WWTP secondary effluent. This effect is further confirmed by the kinetic rate constants presented in Table 6, which exhibit a significant reduction compared to the MCPA treatment in the ultrapure water. Despite the effect of carbonates and organic matter on the medium, the MCPA conversion was above 70% in all cases, demonstrating the potential of solar photo-Fenton as a polishing tertiary treatment in WWTP effluents.

Table 6. Apparent kinetic rate constants and specific rate constants for MCPA degradation in the water matrix assessment.

Matrix	$k_{app,MCPA}$ (min^{-1}) × 10^2	r^2
Ultrapure water	3.34	0.96
River water	2.48	0.95
WWTP effluent	2.23	0.98

4. Conclusions

The solar photo-Fenton process is a feasible technology for the degradation of MCPA in the aqueous phase. Preliminary tests showed the synergic effect of introducing solar radiation on both MCPA depletion and H_2O_2 consumption. The presence of dissolved O_2 in the reaction medium significantly enhanced the mineralization efficiency of both the target pollutant and its degradation byproducts, facilitating a more complete and sustainable oxidative process. A parametric study identified pH_0 as the most critical variable influencing the system's performance, due to iron complexation and precipitation, diminishing the catalyst availability. Under optimized conditions (presence of dissolved oxygen in the medium, $[Fe^{2+}]$: 7.50 mg/L, $[H_2O_2]_0$: 322 mg/L (stoichiometric dose), pH_0 ≈ 3.5), complete MCPA removal was achieved after 30 min, with a 98.40% mineralization degree attained after 180 min. Under stoichiometric doses of the H_2O_2, this process primarily generated biodegradable byproducts, mainly short-chain acids, resulting in a significant reduction in toxicity, as verified through phytotoxicity and ecotoxicity tests. After the study of the process at a high MCPA concentration (100 mg/L), the process feasibility was tested in relevant matrices (river water and WWTP secondary effluent), at a more relevant MCPA concentration (100 µg/L), with $X_{MCPA} \geq 70\%$ in all cases after 60 min

reaction. Hence, solar photo-Fenton arises as a promising technology for the elimination of chlorinated pesticides such as MCPA.

Author Contributions: A.M.-M.: investigation, methodology, formal analysis validation, writing—original draft, A.M.Z.: methodology, investigation, G.P.: writing: review and editing, J.A.C.: conceptualization, supervision, validation, writing: review and editing, A.L.G.-C.: conceptualization, formal analysis, supervision, writing: review and editing, funding acquisition. All authors have read and agreed to the published version of the manuscript.

Funding: This research was funded by Spanish Agencia Estatal de Investigación, project number project PID2022-139810OA-I00, cofounded through FEDER-EU. A. L. Garcia-Costa thanks Comunidad de Madrid for the Cesar Nombela grant 2023-T1/ECO-29062.

Data Availability Statement: The original contributions presented in this study are included in the article. Further inquiries can be directed to the corresponding author.

Conflicts of Interest: The authors declare no conflicts of interest.

Appendix A

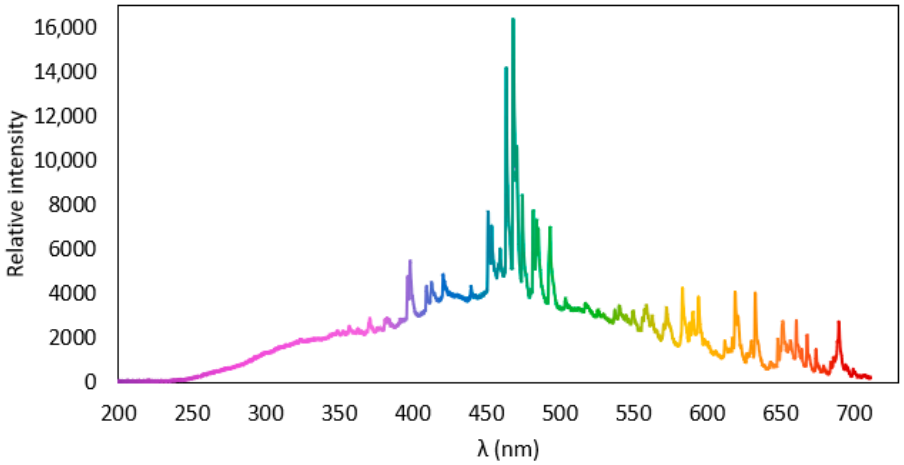


Figure A1. Emission spectrum of the T-Xe lamp.

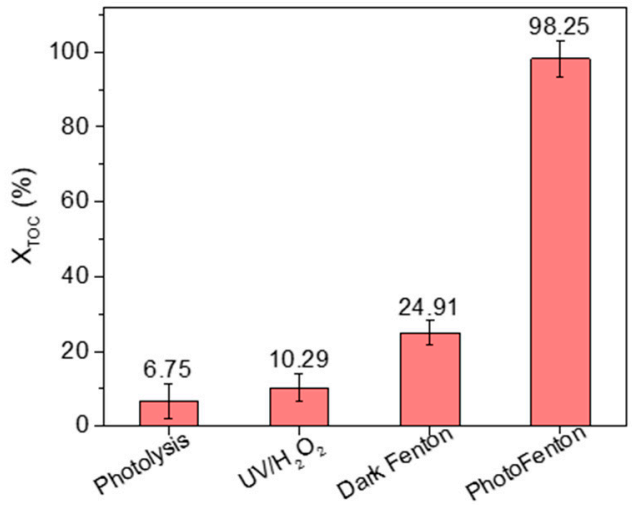


Figure A2. TOC removal for process screening at 180 min. Operating conditions: $[MCPA]_0$ = 100 mg/L, $[H_2O_2]_0$ = 322 mg/L (100% stoichiometric), $[Fe^{2+}]$: 7.5 mg/L, pH_0: 3.5, T: 25 °C.

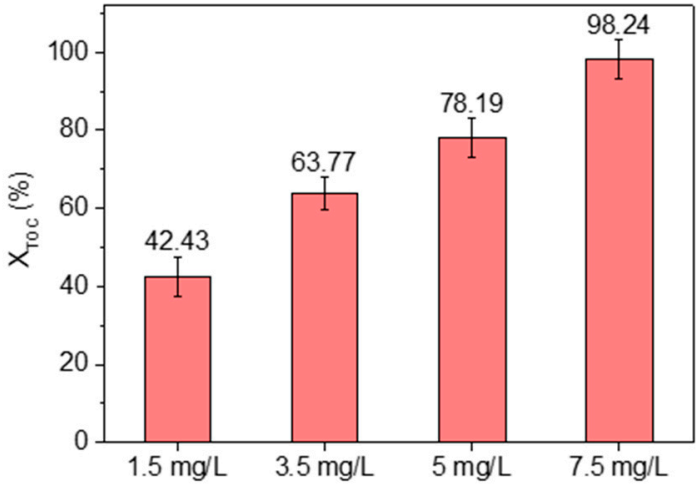


Figure A3. TOC removal for catalyst concentration study at 120 min. Operating conditions: $[MCPA]_0$ = 100 mg/L, $[H_2O_2]_0$ = 322 mg/L (100% stoichiometric), pH_0: 3.5, T: 25 °C, t: 120 min.

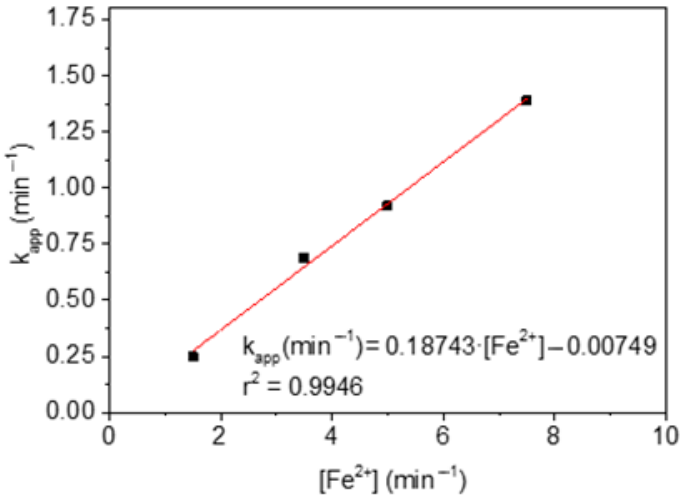


Figure A4. Correlation between $[Fe^{2+}]$ (mg/L) and kinetic apparent kinetic constant (min^{-1}). Operating conditions: $[MCPA]_0$: 100 mg/L, $[H_2O_2]_0$: 322 mg/L (100% stoichiometric), pH_0 = 3.5, T: 25 °C, t: 120 min.

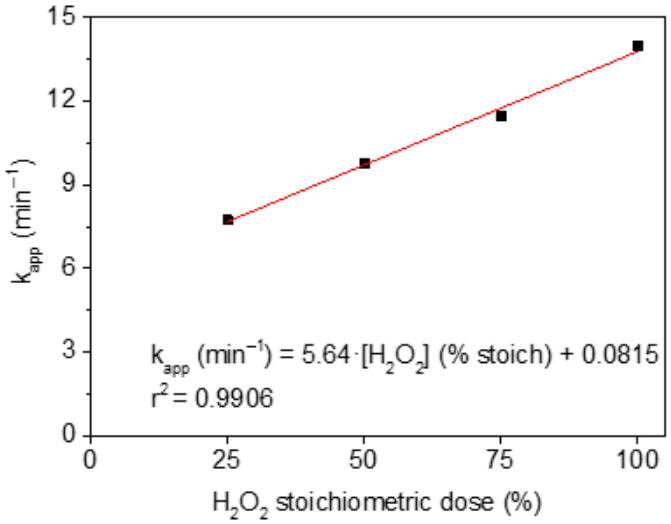


Figure A5. Correlation between H_2O_2 dosage (% stoich) and apparent kinetic constant min^{-1}). Operating conditions: $[MCPA]_0$: 100 mg/L, $[Fe^{2+}]_0$: 7.5 mg/L, pH_0: 3.5, T: 25 °C.

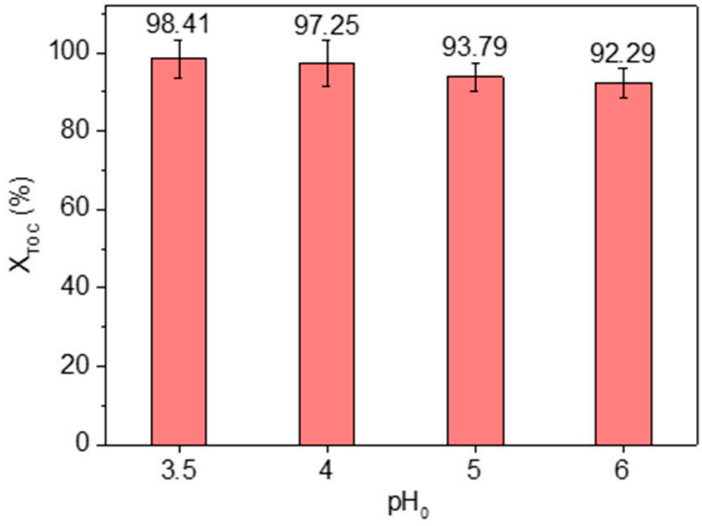


Figure A6. TOC removal for pH_0 study. Operating conditions: $[MCPA]_0$: 100 mg/L, $[H_2O_2]_0$: 322 mg/L (100% stoichiometric), $[Fe^{2+}]$: 7.5 mg/L, t: 120 min, T: 25 °C.

Table A1. Aqueous matrices' characterization.

	River Water	WWTP Effluent
pH	8.11	7.24
Conductivity (μS/cm)	322	599
TOC (mg/L)	0.2	8.55
IC (mg/L)	42.38	14.36
F^- (mg/L)	0.07	0.13
Cl^- (mg/L)	16.09	87.72
NO_3^- (mg/L)	31.35	46.89
SO_4^{2-} (mg/L)	11.30	34.79

References

1. Khan, B.A.; Nadeem, M.A.; Nawaz, H.; Amin, M.M.; Abbasi, G.H.; Nadeem, M.; Ali, M.; Ameen, M.; Javaid, M.M.; Maqbool, R.; et al. Pesticides: Impacts on Agriculture Productivity, Environment, and Management Strategies. In *Emerging Contaminants and Associated Treatment Technologies*; Springer: Berlin/Heidelberg, Germany, 2023; pp. 109–134. [CrossRef]
2. Saleh, I.A.; Zouari, N.; Al-Ghouti, M.A. Removal of pesticides from water and wastewater: Chemical, physical and biological treatment approaches. *Environ. Technol. Innov.* **2020**, *19*, 101026. [CrossRef]
3. Morton, P.A.; Fennell, C.; Cassidy, R.; Doody, D.; Fenton, O.; Mellander, P.; Jordan, P. A review of the pesticide MCPA in the land-water environment and emerging research needs. *Wiley Interdiscip. Rev. Water* **2019**, *7*, e1402. [CrossRef]
4. Gong, T.; Gao, C.; Ji, S.; Xing, Y. Efficient degradation of MCPA in water by light/MIL-88A/H_2O_2 system: Mechanism, degradation pathways and toxicity assessment. *J. Water Process Eng.* **2024**, *64*, 105687. [CrossRef]
5. Ministerio para la Transición Ecológica y el Reto Demográfico. *Informe de Resultados de la Campaña de Muestreo 2023: Red de Detección del Riesgo por Plaguicidas*; Dirección General del Agua: Madrid, Spain, 2024. Available online: https://www.miteco.gob.es/ (accessed on 2 May 2025).
6. Gogate, P.R.; Pandit, A.B. A review of imperative technologies for wastewater treatment I: Oxidation technologies at ambient conditions. *Adv. Environ. Res.* **2003**, *8*, 501–551. [CrossRef]
7. Miklos, D.B.; Remy, C.; Jekel, M.; Linden, K.G.; Drewes, J.E.; Hübner, U. Evaluation of advanced oxidation processes for water and wastewater treatment—A critical review. *Water Res.* **2018**, *139*, 118–131. [CrossRef]
8. Oturan, M.A.; Aaron, J. Advanced Oxidation Processes in Water/Wastewater Treatment: Principles and Applications. A Review. *Crit. Rev. Environ. Sci. Technol.* **2014**, *44*, 2577–2641. [CrossRef]
9. Quan, Y.; Zhao, P.; Chen, L. Kinetics of ozonation of 4-Chloro-2-Methyl phenoxyacetic acid in aqueous solution. *Proc. Int. Conf. Remote Sens. Environ.* **2012**, *43*, 1–4. [CrossRef]
10. Benitez, F.J.; Acero, J.L.; Real, F.J.; Roman, S. Oxidation of MCPA and 2,4-D by UV Radiation, Ozone, and the Combinations UV/H_2O_2 and O_3/H_2O_2. *J. Environ. Sci. Health B* **2004**, *39*, 393–409. [CrossRef]

11. Quiñones, D.; Rey, A.; Álvarez, P.; Beltrán, F.; Puma, G.L. Boron doped TiO_2 catalysts for photocatalytic ozonation of aqueous mixtures of common pesticides: Diuron, o-phenylphenol, MCPA and terbuthylazine. *Appl. Catal. B Environ.* **2014**, *178*, 74–81. [CrossRef]
12. Azarpira, H.; Rasolevandi, T.; Mahvi, A.H. 4-Chloro-2-methylphenoxyacetic acid decomposition by production of reduction species in sulfite excitation through photolysis. *J. Mol. Struct.* **2024**, *1316*, 138927. [CrossRef]
13. Pignatello, J.J.; Oliveros, E.; MacKay, A. Advanced Oxidation Processes for Organic Contaminant Destruction Based on the Fenton Reaction and Related Chemistry. *Crit. Rev. Environ. Sci. Technol.* **2006**, *36*, 1–84. [CrossRef]
14. Babuponnusami, A.; Muthukumar, K. A review on Fenton and improvements to the Fenton process for wastewater treatment. *J. Environ. Chem. Eng.* **2014**, *2*, 557–572. [CrossRef]
15. Munter, R. Advanced oxidation processes—Current status and prospects. *Proc. Estonian Acad. Sci. Chem.* **2001**, *50*, 59–80. [CrossRef]
16. Marchetti, M.D.; Azevedo, E.B. Degradation of NSAIDs by optimized photo-Fenton process using UV-LEDs at near-neutral pH. *J. Water Process Eng.* **2020**, *35*, 101171. [CrossRef]
17. Blanco-Galvez, J.; Fernández-Ibáñez, P.; Malato-Rodríguez, S. Solar Photocatalytic Detoxification and Disinfection of Water: Recent Overview. *J. Sol. Energy Eng.* **2006**, *129*, 4–15. [CrossRef]
18. MacAdam, J.; Parsons, S.A. An investigation into advanced oxidation of three chlorophenoxy pesticides in surface water. *Water Sci. Technol.* **2009**, *59*, 1665–1671. [CrossRef]
19. Brillas, E.; Boye, B.; Dieng, M.M. General and UV-Assisted Cathodic Fenton Treatments for the Mineralization of Herbicide MCPA. *J. Electrochem. Soc.* **2003**, *150*, E583. [CrossRef]
20. Bressan, M.; Liberatore, L.; D'Alessandro, N.; Tonucci, L.; Belli, C.; Ranalli, G. Improved Combined Chemical and Biological Treatments of Olive Oil Mill Wastewaters. *J. Agric. Food Chem.* **2004**, *52*, 1228–1233. [CrossRef]
21. Malato, S.; Fernández-Ibáñez, P.; Maldonado, M.; Blanco, J.; Gernjak, W. Decontamination and disinfection of water by solar photocatalysis: Recent overview and trends. *Catal. Today* **2009**, *147*, 1–59. [CrossRef]
22. Bernabeu, A.; Vercher, R.; Santos-Juanes, L.; Simón, P.; Lardín, C.; Martínez, M.; Vicente, J.; González, R.; Llosá, C.; Arques, A.; et al. Solar photocatalysis as a tertiary treatment to remove emerging pollutants from wastewater treatment plant effluents. *Catal. Today* **2010**, *161*, 235–240. [CrossRef]
23. Zhang, T.; Wang, X.; Zhang, X. Recent Progress in TiO_2-Mediated Solar Photocatalysis for Industrial Wastewater Treatment. *Int. J. Photoenergy* **2014**, *2014*, 607954. [CrossRef]
24. Gutierrez-Mata, A.G.; Velazquez-Martínez, S.; Álvarez-Gallegos, A.; Ahmadi, M.; Hernández-Pérez, J.A.; Ghanbari, F.; Silva-Martínez, S. Recent Overview of Solar Photocatalysis and Solar Photo-Fenton Processes for Wastewater Treatment. *Int. J. Photoenergy* **2017**, *2017*, 8528063. [CrossRef]
25. Bauer, R.; Fallmann, H. The Photo-Fenton Oxidation—A Cheap and Efficient Wastewater Treatment Method. *Res. Chem. Intermed.* **1997**, *23*, 341–354. [CrossRef]
26. Eisenberg, G. Colorimetric Determination of Hydrogen Peroxide. *Ind. Eng. Chem. Anal. Ed.* **1943**, *15*, 327–328. [CrossRef]
27. *ISO 18763:2016*; Soil Quality—Determination of the Toxic Effects of Pollutants on Germination and Early Growth of Higher Plants. International Organization for Standardization: Geneva, Switzerland, 2016.
28. *ISO 11348-3*; Water Quality—Determination of the Inhibitory Effect of Water Samples on the Light Emission of Vibrio fischeri (Luminescent bacteria Test)—Part 3: Method Using Freeze-Dried Bacteria. International Organization for Standardization: Geneva, Switzerland, 1998.
29. Hao, O.J.; Lin, C.F.; Jeng, F.T.; Shih, C.J. A review of Microtox test and its applications. *Toxicol. Environ. Chem.* **1995**, *52*, 57–76. [CrossRef]
30. Zazo, J.A.; Casas, J.A.; Molina, C.B.; Quintanilla, A.; Rodriguez, J.J. Evolution of Ecotoxicity upon Fenton's Oxidation of Phenol in Water. *Environ. Sci. Technol.* **2007**, *41*, 7164–7170. [CrossRef] [PubMed]
31. Olak-Kucharczyk, M.; Ledakowicz, S. Advanced oxidation of preservative agents in H_2O_2/UVC system—Kinetics study, transformation products and toxicity assessment. *J. Hazard. Mater.* **2017**, *333*, 348–357. [CrossRef]
32. Garcia-Costa, A.L.; Lopez-Perela, L.; Pliego, G.; Zazo, J.A.; Casas, J.A. Effective degradation of cyclohexanecarboxylic acid by visible LED driven photo-Fenton. *Chem. Eng. J. Adv.* **2021**, *9*, 100198. [CrossRef]
33. Von Sonntag, C.; Dowideit, P.; Fang, X.; Mertens, R.; Pan, X.; Schuchmann, M.N.; Schuchmann, H. The fate of peroxyl radicals in aqueous solution. *Water Sci. Technol.* **1997**, *35*, 9–15. [CrossRef]
34. Vallejo, M.; Fernández-Castro, P.; Román, M.F.S.; Ortiz, I. Assessment of PCDD/Fs formation in the Fenton oxidation of 2-chlorophenol: Influence of the iron dose applied. *Chemosphere* **2015**, *137*, 135–141. [CrossRef]
35. Ribeiro, J.P.; Marques, C.C.; Portugal, I.; Nunes, M.I. Fenton processes for AOX removal from a kraft pulp bleaching industrial wastewater: Optimisation of operating conditions and cost assessment. *J. Environ. Chem. Eng.* **2020**, *8*, 104032. [CrossRef]
36. Muñoz, M.; De Pedro, Z.M.; Pliego, G.; Casas, J.A.; Rodriguez, J.J. Chlorinated Byproducts from the Fenton-like Oxidation of Polychlorinated Phenols. *Ind. Eng. Chem. Res.* **2012**, *51*, 13092–13099. [CrossRef]

37. Potter, F.J.; Roth, J.A. Oxidation of Chlorinated Phenols Using Fenton's Reagent. *Hazard. Waste Hazard. Mater.* **1993**, *10*, 151–170. [CrossRef]
38. González, O.; Sans, C.; Esplugas, S. Sulfamethoxazole abatement by photo-Fenton: Toxicity, inhibition and biodegradability assessment of intermediates. *J. Hazard. Mater.* **2007**, *146*, 459–464. [CrossRef] [PubMed]
39. Clarizia, L.; Russo, D.; Di Somma, I.; Marotta, R.; Andreozzi, R. Homogeneous photo-Fenton processes at near neutral pH: A review. *Appl. Catal. B Environ.* **2017**, *209*, 358–371. [CrossRef]
40. Bulich, A.A. A practical and reliable method for monitoring the toxicity of aquatic samples. *Process Biochem.* **1982**, *17*, 45–47.
41. Neamţu, M.; Grandjean, D.; Sienkiewicz, A.; Le Faucheur, S.; Slaveykova, V.; Velez Colmenares, J.J.; Pulgarin, C.; de Alencastro, L.F. Degradation of eight relevant micropollutants in different water matrices by neutral photo-Fenton process under UV254 and simulated solar light irradiation—A comparative study. *Appl. Catal. B Environ.* **2014**, *158–159*, 30–37. [CrossRef]
42. Cheng, X.; Liang, L.; Ye, J.; Li, N.; Yan, B.; Chen, G. Influence and mechanism of water matrices on H_2O_2-based Fenton-like oxidation processes: A review. *Sci. Total Environ.* **2023**, *888*, 164086. [CrossRef]
43. Bautitz, I.R.; Nogueira, R.F.P. Degradation of tetracycline by photo-Fenton process—Solar irradiation and matrix effects. *J. Photochem. Photobiol. A Chem.* **2006**, *187*, 33–39. [CrossRef]
44. Grebel, J.E.; Pignatello, J.J.; Mitch, W.A. Effect of Halide Ions and Carbonates on Organic Contaminant Degradation by Hydroxyl Radical-Based Advanced Oxidation Processes in Saline Waters. *Environ. Sci. Technol.* **2010**, *44*, 6822–6828. [CrossRef]
45. Xiao, R.; Meng, Y.; Fu, Y.; Wacławek, S.; Wei, Z.; Spinney, R.; Dionysiou, D.D.; Zeng, W.; Hu, W. The overlooked carbonate radical in micropollutant degradation: An insight into hydration interaction. *Chem. Eng. J.* **2023**, *474*, 145245. [CrossRef]

Disclaimer/Publisher's Note: The statements, opinions and data contained in all publications are solely those of the individual author(s) and contributor(s) and not of MDPI and/or the editor(s). MDPI and/or the editor(s) disclaim responsibility for any injury to people or property resulting from any ideas, methods, instructions or products referred to in the content.